Magnetizing Inrush Current Elimination Strategy Based on a Parallel Type Asynchronous Closing Hybrid Transformer

Zhiwei Chen, *Member, IEEE*, Haonan Li, Xiaofei Dong, Yunxiang He, Qipei Zhou, Yujiao Zhang, *Member, IEEE*, and Yingying Zhang, *Member, IEEE*

***Abstract*—When the power transformer is connected to power grids, due to the existing remanent magnetism (RM) and the voltage transient component, the transformer will generate a large magnetizing inrush current (MIC). The MIC not only seriously threatens the safe operation of the transformer, but also causes the misoperation in the differential protections. To solve the aforementioned problems, a novel MIC elimination strategy of the hybrid transformer (HT) based on an asynchronous closing technology is proposed in this article. First, through the rational design of the HT topology, the parallel auxiliary winding (PAW) of the HT is established and the magnetic coupling mechanism is realized, which lay the magnetic circuit foundation for the MIC management. Second, a step-type synchronous magnetic field is established through PAW without considering RM. After the action of step-type magnetic field, the core flux increases sinusoidal linearly and enters into the rated steady stable. Finally, by controlling the stabilization time of the oblique wave and the primary voltage signal of the power grid, when the core flux is stabilized, the nonsynchronous closing of the HT can effectively alleviate the generation of the MIC. The validity and feasibility of the proposed scheme are verified by building an HT prototype platform, which provides some reference for the difficulty of measuring RM and avoiding MIC in the power system.**

***Index Terms*—Asynchronous closing, hybrid transformer (HT), magnetizing inrush current (MIC), remanent magnetism (RM).**

I. Introduction

POWER transformers are an important part of the power system. Their normal working state decide directly the quality of electric energy. When the transformer is connected to the power grid without load, the remanent magnetism (RM) of the transformer and the transient component of the voltage will lead to the iron core saturation of transformers and generate a huge magnetizing inrush current (MIC). The MIC is usually 6–8 times bigger than the rated current. Under normal circumstances, because the inrush current has a short of duration time and it cannot result in severe harm for the transformer itself, but long-term and repeated MIC may cause the transformer winding to loose, which will reduce the transformer life, as in [1] and [2]. Moreover, the magnetic flux with many harmonic wave in the transformer can lead to the transformer secondary-side voltage distortion and the inverter commutation failure, which will affect the normal working of the inverter. When the transformer generates a large MIC, if the differential protection (DP) could not identify the MIC, it will be misjudged as a short-circuit current, which will lead to the maloperation of a busbar DP, resulting in a large area of power cut. Moreover, the MIC including a lot of harmonic wave results in magnetic circuit oversaturation of the current transformers and reduces the measurement accuracy of the current transformers, as in [3], [4], [5].

At present, the research of the MIC mainly focuses on the identification methods. For example, the identification methods based on the currents have the second harmonics method, the virtual third harmonic principle, and the dead-angle principle. The identification methods based on the voltage angle have the wavelet theory method, as in [6] and [7], the fuzzy theory, the neural network method, etc., as in [8], [9], [10]. The aforementioned methods all belong to the MIC identification method, which can be realized to a certain extent, and the DP device does not operate. However, none of these methods can fundamentally eliminate the MIC. Jazebi et al. [11] proposed that the series resistance of the main circuit can effectively reduce the peak value of the MIC and greatly shorten the duration of the MIC, but the MIC cannot be eliminated. Samantaray [12] adopted the phase-selective closing strategy, whose main idea is that the magnetic flux generated by the voltage is opposite to RM of the transformer. Based on this principle, the purpose of three-phase transformer MIC suppression is achieved. But RM measurement is difficult in actual operation. Lu et al. [13] proposed a transformer MIC suppression method based on sinusoidal pulsewidth modulation (SPWM). The strategy of simultaneous closing can be used to effectively suppress the MIC, but the modulation function of the excitation voltage is too complex, which is not conducive to the generation of the pulsewidth modulation (PWM) signal. Over all, the common suppression of the MIC

Manuscript received 27 February 2022; revised 13 April 2022 and 10 June 2022; accepted 19 July 2022. Date of publication 3 August 2022; date of current version 10 October 2022. This work was supported in part by the National Natural Science Foundation of China under Grant 51807044 and Grant 52077048 and in part by the 111 Project under Grant BP0719039. Recommended for publication by Associate Editor A. Safaee. *(Corresponding authors: Zhiwei Chen; Yujiao Zhang.)*

The authors are with the Anhui Province Key Laboratory of Renewable Energy Utilization and Energy Saving, Hefei University of Technology, Hefei 230009, China (e-mail: chenzw_sygd@126.com; 2021170537@mail.hfut.edu.cn; 2019110378@mail.hfut.edu.cn; 2021110330@mail.hfut.edu.cn; 2020170514@mail.hfut.edu.cn; zhangyujiao@hfut.edu.cn; zhangyy@hfut.edu.cn).

Color versions of one or more figures in this article are available at https://doi.org/10.1109/TPEL.2022.3196229.

Digital Object Identifier 10.1109/TPEL.2022.3196229

mainly includes the series resistance of main circuit, the selective phase closing strategy, and the soft start methods, as in [14], [15], etc. These methods are summarized as follows:

A. Series Resistance of the Main Circuit

A series resistance is connected between the input of the transformer and the power grid. When the transformer is connected to the power grid without load, the peak value of the MIC can be effectively reduced and the duration of the MIC can be greatly shortened. When the primary-side current of the transformer reaches the steady state, the resistance can be short-circuited so that the transformer can be directly connected to the power grid. The method has a certain effect on the MIC suppression, but its economic aspect is poor. The higher the voltage grade of the transformer is, the higher the cost of the installation resistance will be.

B. Phase-Selective Closing Strategy

The principle of the phase-selective closing strategy is that the magnetic flux generated by the voltage and RM of the transformer are opposite to each other when closing, and only the steady-state magnetic flux generated by the voltage is left in the iron core. Based on this principle, the suppression purpose of the three-phase transformer MIC is realized. The main closing strategies include the following:

1) *Fast closing strategy*: If the RM of the three-phase iron core are $\Phi_{\rm ra}=0$, $\Phi_{\rm rb}=-0.8\Phi_{\rm m}$, and $\Phi_{\rm rc}=0.8\Phi_{\rm m}$ for a three-phase transformer, where $\Phi_{\rm m}$ *is* the stable magnetic flux, when the initial phase of the phase A voltage $\alpha=k\pi$, where $k=01\ldots$ when the phase A winding is connected to the grid, the magnetic flux of the phase A iron core enters into steady state directly. The dynamic magnetic flux (DMF) of the phase A iron core is $\Phi_A=\Phi_m\sin(\omega t+\alpha)$, and because the circuit breaker of phases B and C is not closed, the magnetic flux in the core of phases B and C is generated only by the voltage of the phase A. The preinduced magnetic flux (PIMF) of phases B and C core will be $\Phi_{\rm B1}=-1/\{2\Phi_{\rm m}\sin(\omega t+\alpha)\}+\Phi_{\rm rb}$ and $\Phi_{\rm C1}=-1/\{2\Phi_{\rm m}\sin(\omega t+\alpha)\}+\Phi_{\rm rc}$. At this time, the DMF generated by the phases B and C is, respectively, $\Phi_{\rm B}=\sqrt{}_{\rm m}\sin(\omega t+\alpha\text{-}2\pi/3)$ and $\Phi_{\rm C}=\Phi_{\rm m}\sin(\omega t+\alpha+2\pi/3)$. When the PIMF of the phases B and C is same as the DMF, closing phases B and C circuit breakers, it will directly enter steady state, and the primary side of the transformer will not generate MIC.
2) *Synchronous closing strategy*: The strategy is a typical closing strategy under the RM pattern. When RM of one phase is 0, RM of the other two phases is equal in magnitude and opposite in direction. If RM of the phase A iron core is 0, when the voltage of the phase A reaches the maximum value, the phase A directly enters the steady state without generating the MIC after closing the primary-side circuit breaker. The DMF generated by the phase B voltage is $\Phi_{\rm B}=\Phi_{\rm m}\sin(\omega t+\langle\text{-}2\pi/3)$, when the DMF produced by the phase B is same as the RM of the phase B iron core, the phase B will directly enter the steady state without generating the MIC. The situation of the phase C magnetic flux is also similar to that of the phase B.
3) *Delay closing strategy*: This method is suitable for transforms with RM in three phases, and the RM amount of one phase is required to be known. It is assumed that RM of the phase A is known, and the circuit breaker of the phase A is closed at the best closing point. The phase A directly enters the steady state without generating the MIC. Under the action of the magnetic balance effect, RM of B and C phases is eliminated. After several cycles, the MIC of B and C phases can be eliminated by B and C phases winding.

The aforementioned phase-selective closing strategy can eliminate the three-phase MIC and make the three-phase winding directly enter the steady state, but it is required to accurately measure the RM of the three phases A, B, and C and determine the closing time at a certain fixed point. Since the circuit breaker closing is discrete, when the circuit breaker has a delay of 1 ms, the angle has deviated 18°. When the circuit breaker has a long delay, the angle deviation is too large. The effect of MIC suppressing will be greatly reduced.

C. Method of Soft Star

This method of transformer MIC suppressing is based on SPWM, as in [16], [17], [18], [19], the synchronous closing strategy can be used to effectively suppress the MIC. But the modulation function of the excitation voltage is too complicated, which is difficult to generate PWM signals. In addition, another transformer T_2 is needed in the MIC suppressor in the main transformer, which increases the cost of the system.

To solve the aforementioned problems, one kind of HT MIC elimination method based on nonsynchronous closing technology without considering RM is proposed in this article. The RM measurement and prediction can be omitted, and the difficulty in the RM measurement also can be effectively solved. By designing the HT topology integrated with an ac/dc converter, deriving the variation law of the PAW-modulated magnetic flux, and establishing the differential equations, the magnetic flux variation law of the core with the voltage is obtained. The step-type modulation magnetic field (STMMF) generated by PAW can stabilizes the core flux in advance. When the HT core flux is stable, then the nonsynchronous closing operation can avoid the generation of the MIC.

II. Principle and Topology of the HT

Based on the conventional transformers (CTs) and power electronic transformers (PETs) operation characteristics, in recent years, some research teams have proposed the HT structure considering the power conversion and the power quality management ability, and combined the traditional PFT and PET to form the HT. To realize the complementation of advantages among efficiency, function, and cost of equipment. This kind transformer is becoming the focus of current research. Based on requirements of MIC management and the integrated mode of a converter, a parallel magnetic coupling type HT topology

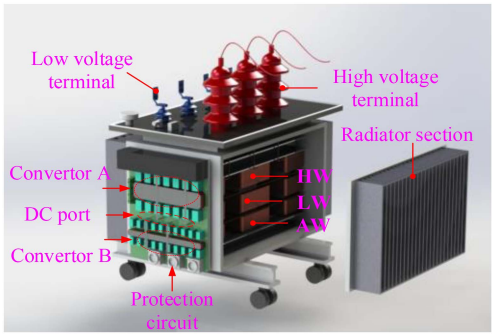

Fig. 1. Schematic diagram of the HT.

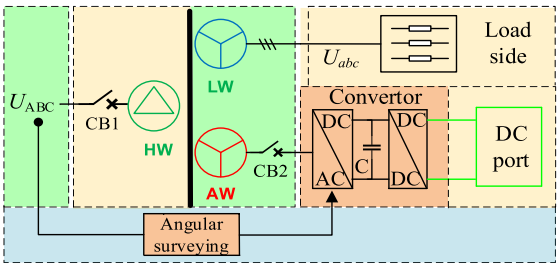

Fig. 2. Circuit diagram of the HT.

is proposed in this article. Fig. 1 is the HT schematic diagram, which includes two parts, two integrated converters and a low-frequency transformer.

In order to solve the transformer MIC problem, a novel parallel magnetic coupling type HT structure is designed in this article. The converter mainly includes two parts, an ac/dc rectifier (converter A) and a dc/dc convertor (converter B), which are mainly used for the rectifier circuit for ac and the voltage conversion for the dc. Fig. 2 is the circuit diagram of the HT. The windings of the HT mainly include the high-voltage winding (HW), the low voltage winding (LW), and the auxiliary winding (AW). U_{ABC} is the three-phase grid voltage, U_{abc} is the three-phase voltage in LW, C is the filter capacitor, and CB1 and CB2 are the high-voltage side and low-voltage side circuit breakers, respectively.

In the HT construction, the AW is used to connect the converter to form the dc port, which can be used to connect the dc load, distributed power supply or energy storage battery to solve the problem of efficient grid-connected operation of renewable energy. The following is a detailed analysis of the matching problem between the AW, HW, and LW winding of the transformer as well as the characteristics of the magnetic circuit topology.

When the HW and LW of HT are open-circuited, and the AW side is supplied with a step-type increasing ac voltage, STMMF of the AW can be established. The total flux of the A-phase iron core is Φ_{ac}. The topology of its mixed magnetic circuit is shown in Fig. 3(a). Among them, U_{A} is the voltage of the phase A on the HW, U_{a} is the voltage of the phase A on the LW, U_{ac} is the voltage of the AW of the phase A on AW, Φ_{A} is the magnetic flux generated by the HW current of the phase A, Φ_{a} is the magnetic flux generated by the LW current of the phase A, Φ_{ac}

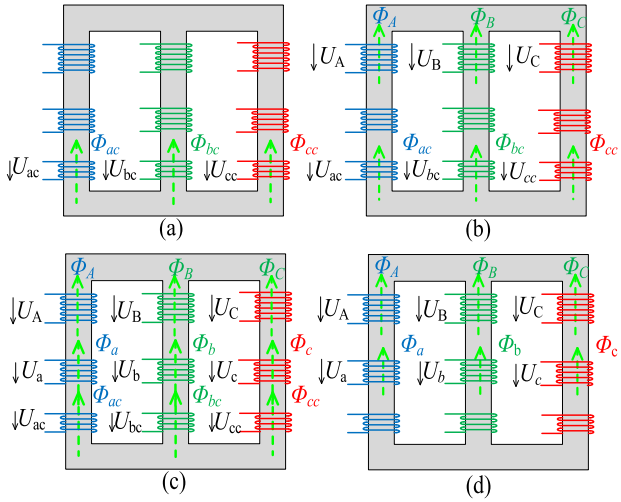

Fig. 3. Magnetic circuit topology of the transformer. (a) STMMF establishment. (b) Transformer closing under no load. (c) Transformer closing with load. (d) AW withdraw.

is the magnetic flux generated by the AW current of the phase A, and the same is true for the winding of phases B and phase C. When the STMMF tends to be stable, the circuit breaker of LW of the transformer is open. The winding currents of the HW and AW jointly establish the magnetomotive force, and the total magnetic flux of the phase A is $\Phi_{\mathrm{A}}+\Phi_{\mathrm{ac}}$, which can realize the no-load closing. The magnetic circuit topology is shown in Fig. 3(b). When the transformer needs to close with load, the HW, LW, and AW currents jointly establish the magnetomotive force. The total magnetic flux of the phase A is $\Phi_{\mathrm{A}}+\Phi_{\mathrm{a}}+\Phi_{\mathrm{ac}}$, and its magnetic circuit topology is shown in Fig. 3(c). When the transformer operates normally, AW can be withdrawn. The HW and LW current jointly establish the magnetomotive force, and the magnetic flux of the phase A is $\Phi_{\mathrm{A}}+\Phi_{\mathrm{a}}$. At this time, HT is in the operation state of the traditional transformer. Its magnetic circuit topology is shown in Fig. 3(d).

III. MIC Management Strategy of Asynchronous Closing HT

When the transformer is closed without load, due to the transient magnetic flux and the RM, the superposition of the magnetic flux may exceed the saturation magnetic flux and a huge MIC will be generated. By controlling the magnitude of the input AW voltage, the magnetic flux is smoothly increased, and the magnetic flux amplitude never exceeds the saturation value, as in [21]. When the magnetic flux is stable, the circuit breaker on the HW can be closed to suppress the generation of the MIC. This method has obvious effects on the MIC suppression. It does not need to measure the size and direction of RM, and can also establish a stable magnetic flux steadily.

The specific implementation method is as follows. The phase of the grid voltage is collected and transmitted to the dc/ac inverter through the phase measurement module so that the alternating voltage output from the dc/ac module is same as the phase in the power grid. The AW is fed with step-type increasing sinusoidal modulated alternating voltage (when the amplitude

of the applied alternating voltage reaches the rated voltage on the AW side, it will no longer increase linearly and keep the amplitude stable). As the voltage amplitude of the AW increases linearly, the magnetic flux will also increase steadily. Choosing a suitable linear slope, and there will be no MIC on the AW side at this time. When stable ac magnetic flux is established in the iron core, and the magnitude of the magnetic flux is same as the magnetic flux of the transformer under the normal operation, the magnetic flux will induce a rated voltage on the primary side. At this time, the amplitude and the phase of the induced voltage in the transformer primary side are same as the voltage amplitude and phase of the power grid. If the circuit breaker on the primary side is closed asynchronously, no MIC will be generated on the primary side. The MIC on the primary side of the transformer can be directly eliminated.

Take a single-phase transformer as an example to analyze the magnetic flux changes in the core. $U_1 = atU_{\mathrm{m}}\cos(\omega t+\alpha)$ is added to the transformer AW side.

$$R_1 i_1 + N_1 \frac{d\phi}{dt} = atU_m \cos(\omega t + \alpha) \tag{1}$$

where L is the equivalent inductance of AW, N_1 is the coil number of AW, R_1 is equivalent resistance, i_1 is the current, ϕ is the magnetic flux, a is the slope of the linear increase, and α is the initial phase of the power grid voltage. $Li_1 = N_1\phi$ and $\phi(0) = \phi_{\mathrm{res}}$, where ϕ_{res} is initial value of the magnetic flux.

The following can be obtained from (1):

$$R_1 \frac{N_1\phi}{L} + N_1 \frac{d\phi}{dt} = atU_m \cos(\omega t + \alpha). \tag{2}$$

After calculation

$$\begin{aligned}\phi = {} & \left\{\phi_{res} - \frac{aLU_m}{N_1\left[R_1^2 + (\omega L)^2\right]^2}(\omega^2 L^3 \cos\alpha \right. \\ & \left. - R_1^2 L\cos\alpha - 2\omega R_1 L^2 \sin\alpha)\right\} e^{\frac{-R_1 t}{L}} \\ & + \frac{aLU_m}{\left[R_1^2 + (\omega L)^2\right]^2 N_1}\{\omega^2 L^3 \cos(\omega t+\alpha) \\ & - R_1^2 L\cos(\omega t+\alpha) + R_1^3 t\cos(\omega t+\alpha) \\ & - 2\omega R_1 L^2 \sin(\omega t+\alpha) + \omega^3 L^3 t\sin(\omega t+\alpha) \\ & + \omega^2 R_1 L^2 t\cos(\omega t+\alpha) + \omega R_1^2 L t\sin(\omega t+\alpha)\}\end{aligned} \tag{3}$$

$$\phi_{\mathrm{m}} = \frac{U_{\mathrm{m}} L}{N_1\sqrt{(R_1^2 + \omega^2 L^2)}}. \tag{4}$$

When $\omega L >> R_1$, the approximate formula for ϕ can be obtained As follows:

$$\phi = \phi_{\mathrm{res}} e^{\frac{-R_1 t}{L}} + at\phi_{\mathrm{m}} \sin(\omega t+\alpha). \tag{5}$$

Further simplified ϕ can be obtained as follows

$$\phi = \phi_{\mathrm{res}} e^{\frac{-R_1 t}{L}} + at\phi_{\mathrm{m}} \tag{6}$$

$$\frac{d\phi}{dt} = \frac{-R_1}{L}\phi_{\mathrm{res}} e^{\frac{-R_1 t}{L}} + a\phi_{\mathrm{m}}. \tag{7}$$

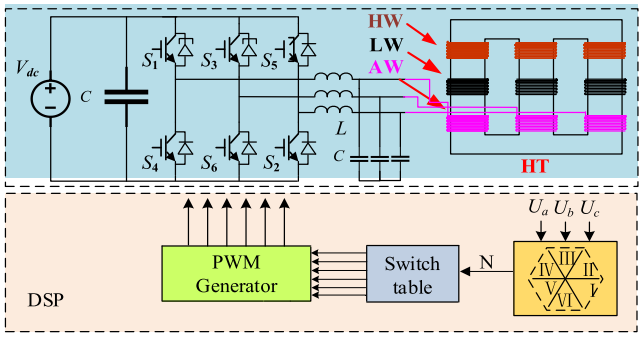

Fig. 4. Three-phase bridge inverter circuit in the HT.

Set the left of (7) equal to 0.

$$t_1 = \frac{-L}{R_1}\ln\frac{a\phi_{\mathrm{m}} L}{R_1\phi_{\mathrm{res}}}. \tag{8}$$

$$m = \frac{a\phi_{\mathrm{m}} L}{R_1\phi_{\mathrm{res}}}. \tag{9}$$

If $0<m<1$, when t is in from 0 to t_1,ϕ decreases. When t is in from t_1 to $1/a$, ϕ increases. That is, $\phi(0)$ or $\phi(1/a)$ is the maximum. If $\phi_{\max} = \phi(0)$, $\phi_{\max} = \phi_{\mathrm{res}}$, the iron core is not saturated and MIC will not appear.

When $\phi_{\max} = \phi(1/a)$

$$\phi_{\max} = \phi_{\mathrm{res}} e^{\frac{-R_1}{aL}} + \phi_{\mathrm{m}}. \tag{10}$$

When $\phi_{\max} = 1.2\phi_{\mathrm{m}}$

$$0 < a < \frac{-R_1}{L}\frac{1}{\ln\frac{0.2\phi_{\mathrm{m}}}{\phi_{\mathrm{res}}}}. \tag{11}$$

When an ac voltage with a stepwise increase amplitude is added to the AW, the magnetic flux at this time is the sum of the RM and the linearly increasing sinusoidal magnetic flux. According to (11), when the slope a is within the range, the MIC could not be generated on the AW side. When the magnetic flux in the iron core becomes stable, a rated voltage with the same amplitude and phase as the grid voltage will be induced in HW, that is, a stable magnetic flux has been established in the iron core. Closing the circuit breaker on the primary side, HW will enter into stable state directly.

IV. Principle and Controlling Strategy of STMMF

According to the requirement of the AW topology, the main circuit of STMMF is designed. The main circuit topology contains the three-phase bridge inverter circuit and NPC three level inverter circuit. The topology of the designed main circuit in this article is shown in Fig. 4.

A. STMMF Building

The main circuit adopts a three-phase bridge inverter circuit and its output voltage will be filtered through the *LCL*, then the filtered alternating voltage is as the input of the AW. In order to control and reduce the current amplitude of AW does not generate an inrush current, the transformer AW needs to input a sinusoidal voltage with a linear increase amplitude. The input

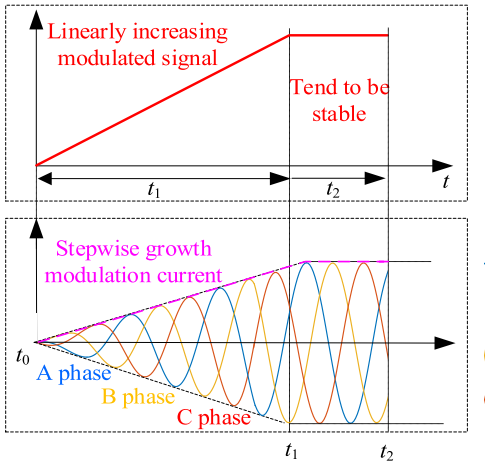

Fig. 5. Generation process of the three-phase modulation voltage.

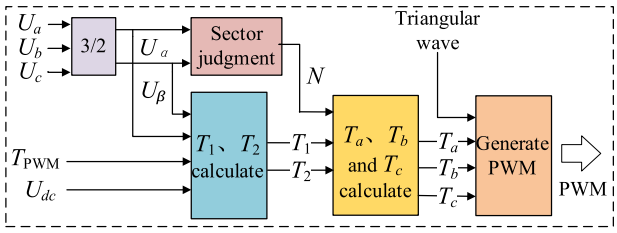

Fig. 6. Simulink simulation generated by PWM.

signal of this article is a ramp function whose slope is a. The amplitude of the input signal increases with the time. If $at \geq 1$, the output always is 1. At this time, connect the output signal to U_d, and connect U_q to 0, $f = 50$ Hz, TPWM $= 100$ s, and $U_{dc} = 100$ V. After the *dq-abc* conversion, the output three-phase sinusoidal signal with a phase difference of 120° will be output. This process is shown in Fig. 5.

From t_0-t_1, the inverter outputs three-phase alternating voltage with a linear increasing amplitude, and the amplitude of the induced magnetic flux also increases. At t_2, the phase B voltage reaches to the rated value. The magnetic flux also reaches to the rated value. Then, the required control signal of MOSFET is generated by using SVPWM. The process of the control signal generation based on SVPWM is shown in Fig. 6.

Based on SVPWM, the PWM controlling signal can be obtained. After extracting the values of U_a, U_b, *and* U_c, the values of T_a, T_b, and T_c can be calculated through the converter of *abc*-$\alpha\beta$. Comparing the isosceles triangle of this picture with the calculated T_a, T_b, and T_c, the corresponding PWM waveform can be obtained. The waveform of PWM_1, PWM_3, and PWM_5 are shown in Fig. 7.

B. Controlling Signal Formation

The program of the controlling signal formation is shown in Fig. 8. The MOSFET control signal required for the MIC elimination experiment is generated based on the principle of SVPWM, the period of the PWM square wave is set as 100 μs, and the dead time of the upper and lower switching tubes of a bridge arm is set as 2μs. A timer interrupt is set every 10 μs. In the interrupt,

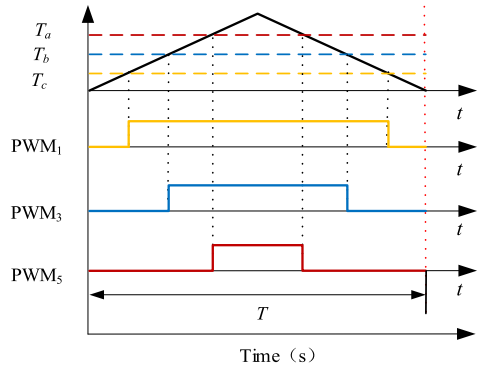

Fig. 7. Generation process of PWM waveform.

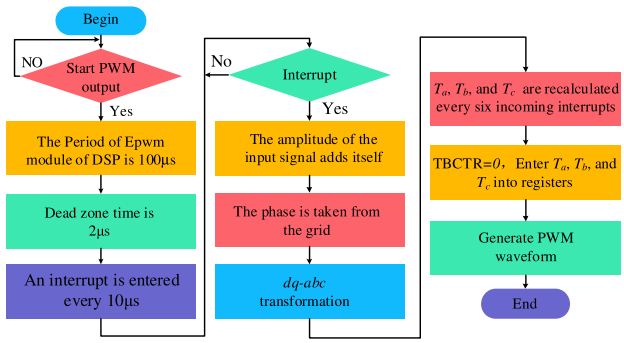

Fig. 8. Flow chart of PWM signal generated by the DSP.

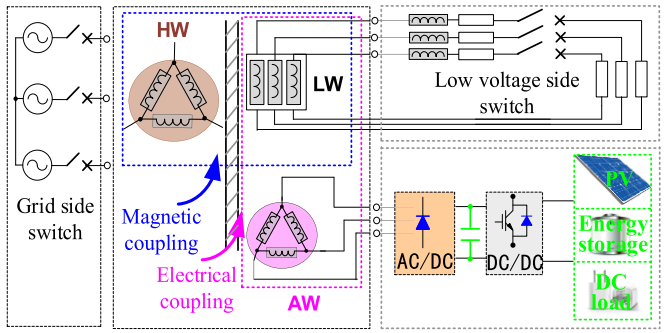

Fig. 9. Simulation schematic diagram of the MIC elimination strategy.

the phase is taken from the grid. The input signal increases linearly, and the input signal is converted into a corresponding three-phase ac signal. T_a, T_b, and T_c are recalculated every six times when the interrupt is triggered. And when the value of epwm module counter (TBCTR) $= 0$, T_a, T_b, and T_c will be imported into the register to output the corresponding PWM waveform.

V. Simulation Verification of Asynchronous Closing HT MIC Elimination Strategy

A. MIC Simulation

To verify the validity of the proposed MIC elimination strategy based on the asynchronous closing HT, the HT model is built in MATLAB/SIMULINK for simulation and verification. The simulation model is shown in Fig. 9.

TABLE I
TRANSFORMER RATING PARAMETERS

Parameter	Numerical value (unit)
Transformer capacity	1kVA
Voltage ratio	220/110/22
R_1 (p.u.)	0.002
L_1 (p.u.)	0.08
R_m	500
Remanence (p.u.)	0.8
Line resistance	0.01

TABLE II
RATED PARAMETERS OF THE THREE-PHASE TRANSFORMER

Parameter	Numerical value (unit)
Transformer capacity	500kVA
Voltage ratio	10000/400/50
R_1 (p.u.)	0.02
L_1 (p.u.)	0.08
R_m	500
RM of phase A, B and C (p.u.)	0.8, 0, -0.8
Line resistance	0.1

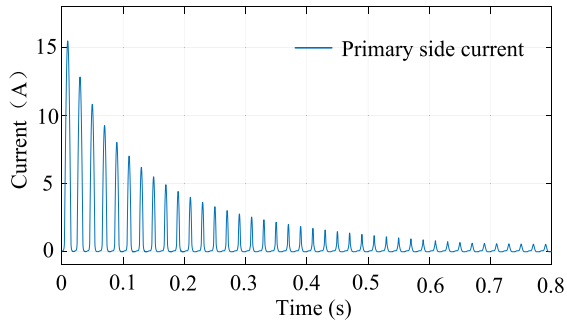

Fig. 10. MIC of primary side of the transformer.

To improve the accuracy of the simulation, a single-phase and three-phase HT are taken as the example, the generation process of the MIC is simulated under the condition of no load and light load. The specific parameters of the single-phase and three-phase HT are shown in Tables I and II.

For the single-phase transformer model, the RM of the transformer is set as $0.8\sqrt{}_{\mathrm{m}}$, and the secondary side as the no load in the simulation. When the voltage phase is 0°, closing the HT primary-side circuit breaker, the current waveform is shown in Fig. 10. At this time, the maximum of current is 16 A. After 12–20 cycles, the current of the primary side become stable and the valid value of the current is 0.018 A.

It should be pointed out that the transformer winding contains resistance and inductance, the closing excitation current will gradually decay, and the speed of decay depends on the time constant *L*/*R*. In generally, for small capacity transformers, the current decays faster and will reach a stable state after about a few cycles. For large-capacity transformers, the attenuation is slow, and some even extend to tens of seconds. The small capacity transformer was used in this manuscript; the excitation current can stabilize in more than ten cycles. According to the rated parameter of the transformer, the primary-side-rated current is about 4.5 A, and no-load current is about 0.4% I_{N}. Now the

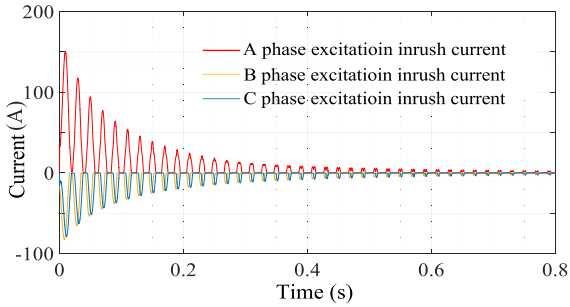

Fig. 11. MIC of primary side of the three-phase transformer.

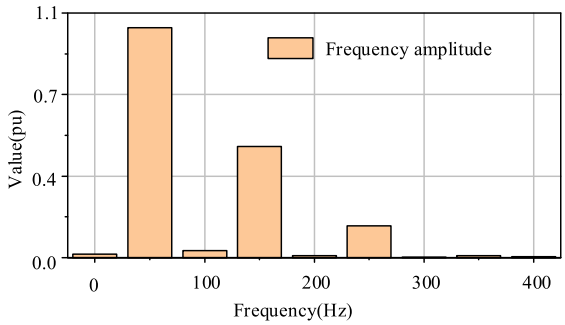

Fig. 12. Harmonic content of MIC on primary side of the single-phase transformer.

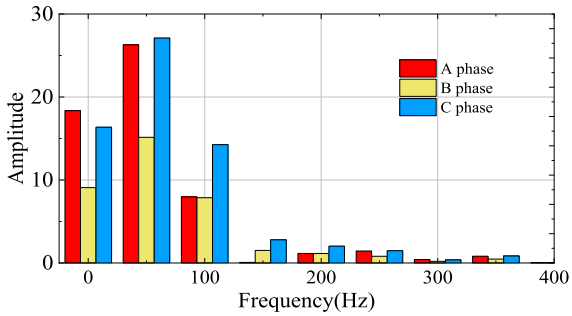

Fig. 13. Harmonic content of MIC on primary side of the three-phase transformer.

current value $i_{\max} = 3.56I_{\mathrm{N}}$, the maximum of current far exceeds the primary-side-rated current.

For the three-phase transformer model, the transformer parameters and RM are shown in Table II. After the simulation model calculation, the maximum of current is 150 A, and the rated current of the three-phase transformer is 16.67 A. The current value $i_{\max} = 8.998I_{\mathrm{N}}$, the maximum of current far exceeds the primary-side-rated current. The three-phase transformer current is shown in Fig. 11.

Fourier decomposition of the no-load current shows that the total harmonic distortion of the primary side is 47.83%, and the amplitudes of each frequency are shown in Fig. 12. In the MIC, the current not only contains the fundamental frequency of 50 Hz, but also contains numbers of higher harmonics and dc components. The amplitude of each frequency of the three-phase transformer is shown in Fig. 13. In addition to the fundamental frequency, the dc component and the second harmonic are the most.

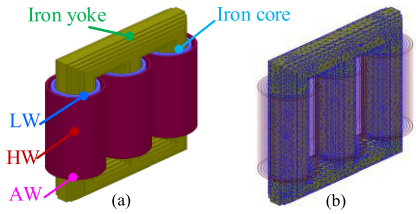

Fig. 14. Simplified electromagnetic model of the three-phase HT.

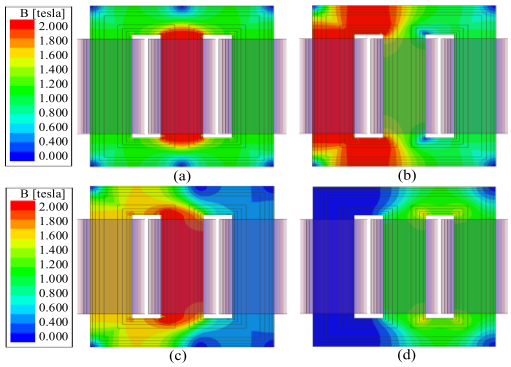

Fig. 15. Magnetic induction intensity distribution diagram of iron core.

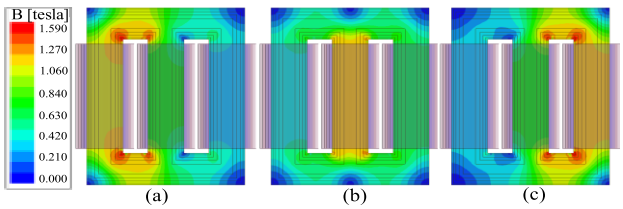

Fig. 16. Magnetic induction intensity distribution diagram of iron core at other closing periods.

Taking the three-phase HT for example, this article uses ANSYS software to build a simplified electromagnetic model of the HT shown in Fig. 14, ignoring the influence of the transformer oil tank and structural components on transformer magnetic circuit distribution. In order to obtain more accurate magnetic flux distribution of the iron core, DW540 is used as the iron core material in this article, double-layer cylindrical winding is used for the HW, LW, and AW, and copper is used as the material. In the simulation software, the HW of the three-phase HT is added to the excitation source, and the corresponding HT core flux distribution map can be obtained. The electromagnetic model and the iron core grid division diagram of the three-phase HT are shown in Fig. 15, and the magnetic induction intensity distribution diagram of the iron core is shown in Fig. 16.

Fig. 15 lists the magnetic induction distribution of the three-phase HT under the different winding saturation conditions. It can be seen from Fig. 15(a) that the magnetic induction intensity of the iron core of phase B winding is about 2T and the MIC occurs in this phase. The magnetic induction intensity of the iron core of phases A and C winding is about 1 T, and no MIC occurs in the aforementioned two phase windings. Fig. 15(b) and (c), respectively, describe the magnetic induction intensity distribution under the saturation of A phase and B phase cores. Fig. 15(d) describes the distribution of magnetic induction

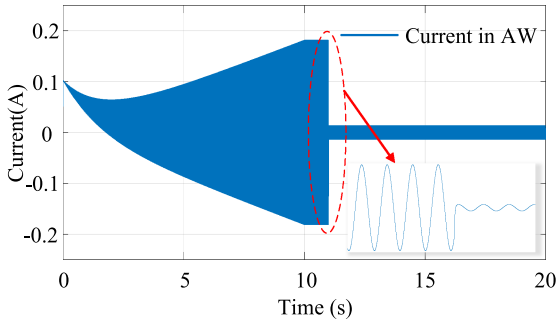

Fig. 17. Current waveform modulated by STMMF in AW of the single-phase HT.

intensity during the normal operation of the HT. At this time, the magnetic induction intensity of phases A, B, and C of the transformer windings is 0.13, 1.2, and 1.1 T, respectively. At this time, there is no MIC occurring in the three windings of the transformer. Fig. 16 shows other closing periods, and it can be seen that no MIC is generated in each phase.

B. MIC Elimination Strategy Based on Asynchronous Closing

When the transition scheme of the asynchronous closing MIC elimination proposed in this article is adopted, RM of the phase A is set as $0.8\Phi_m$ (it can also be set as the values) in the transformer simulation. The sinusoidal alternating voltage with a linear increase amplitude is added to the AW, and the circuit breaker of the primary side is cut off. During 0–10 s, the primary side does not connect to the grid. When the slope a is 0.1, the initial slowly change of the current includes the stepped increase current and the RM attenuation current. Then, the current gradually increase until it is stable at 10 s. The amplitude of the current finally stabilized at 0.18 A, far less than the rated current of the AW. Choose and design the reasonable time of the voltage rise process so that the magnetic flux cannot enter into the excessive saturation area. The current waveform modulated by STMMF in the single-phase AW is shown in Fig. 17. At here, it is assumed that the RM of the three-phase iron core are $\Phi_{\mathrm{ra}} = 0.8\Phi_{\mathrm{m}}$, $\Phi_{\mathrm{rb}} = 0$, and $\Phi_{\mathrm{rc}} = -0.8\Phi_{\mathrm{m}}$ in the process of three-phase transformer simulation. Certainly, the RM value here can also be other values.

The currents waveform modulated by STMMF in the three-phase AW are shown in Fig. 18. Closing the circuit breaker of the primary winding at 10.02 s, the current in AW decreases dramatically soon. According to (10), considering the AW voltage with a linear increase amplitude, the magnetic flux is the superposition of the exponential attenuation RM and the linear increased sine magnetic flux. Equation (11) indicates that if the slope a of the AW is within the allowable range of transformer parameters, the AW also does not generate MIC. When the slope a is set as 10, because the value of the slope exceeds the range allowed of transformer parameters, the current peaks can reach 180 A in the first few cycles. And then, the current rapidly decays and reaches stability at 0.12 s. Closing the breaker of the primary at 0.25 s, the current in AW decreases dramatically

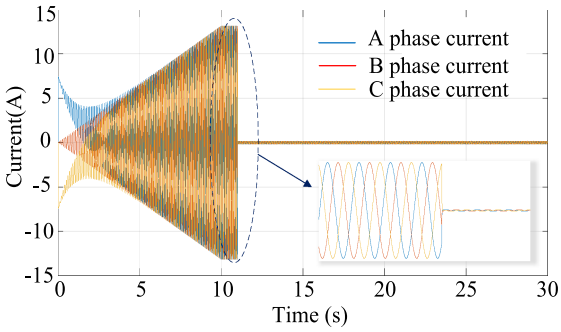

Fig. 18. Current waveform modulated by STMMF in AW of the three-phase HT.

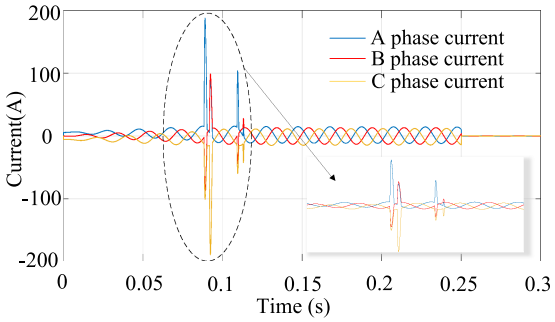

Fig. 19. MIC distribution in AW at the other slope a value.

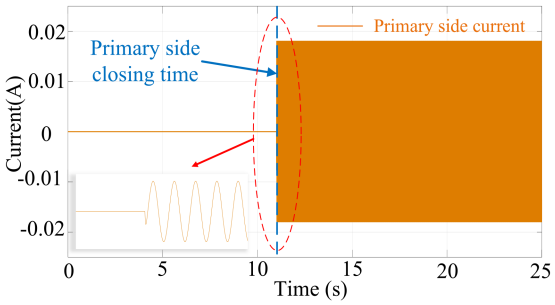

Fig. 20. Excitation current waveform of the HW under the asynchronous closing.

soon. The current waveform of AW is shown in Fig. 19. From to the comparison of the aforementioned two situations, it can be seen that if the value of the slope a is too large and exceeds the range allowed by (11), there will be a large peak current in the AW of the transformer. If the value of the slope a is within the range, there will be no current peak. The current in the AW will gradually reach stability.

It can be seen that at 10 s, the magnetic flux has achieved the stable value. After 10 s, the HW current can directly enter into the stable state when closing the circuit breaker of the primary side, which does not generate any current fluctuations, namely MIC. The primary-side current waveform of the single-phase transformer and three-phase transformer are shown in Figs. 20 and 21. At the same time, the HT proposed in this article can also realize some sensitive voltage sag compensation, and some reactive power compensation and other power quality improvement functions.

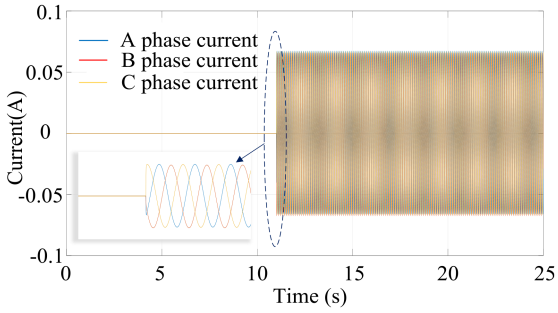

Fig. 21. Excitation current waveform of the HW under the asynchronous closing.

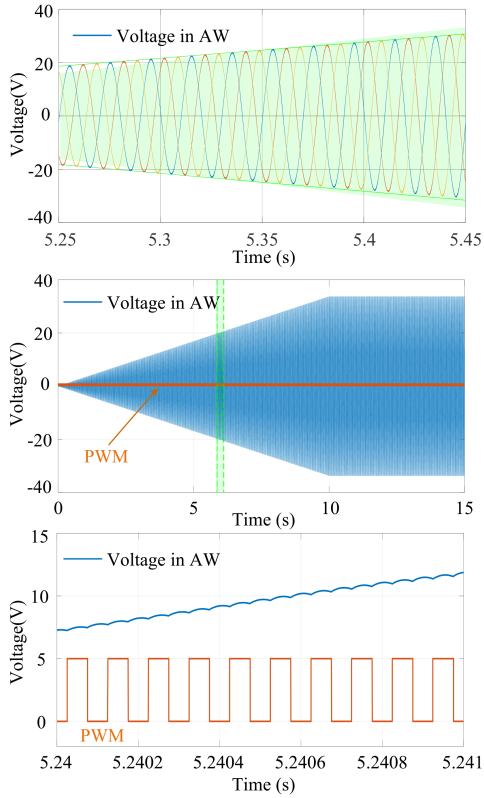

Fig. 22. Voltage distribution and its control signal.

In the simulation process, a sinusoidal modulated ac voltage with an increasing amplitude is added to the HT AW. And locally amplified voltage waveform is shown in Fig. 22(a). The voltage waveform within 0–15s is shown in Fig. 22(b). The control signal and corresponding voltage waveform are shown in Fig. 22(c). The control signals of the three-phase inverter are shown in Fig. 23.

C. Verification of the Validity of the Proposed Scheme

In order to verify the effectiveness of the proposed scheme, this article compares the series resistance of main circuit technology and the phase selective closing strategy. In the simulation, the single-phase transformer and three-phase transformer models are selected. For the series resistance of main circuit technology, a resistor is connected in series at the primary side

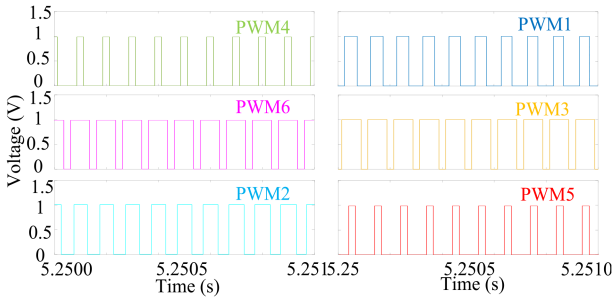

Fig. 23. S_{1-6} Switch control signal of inverter.

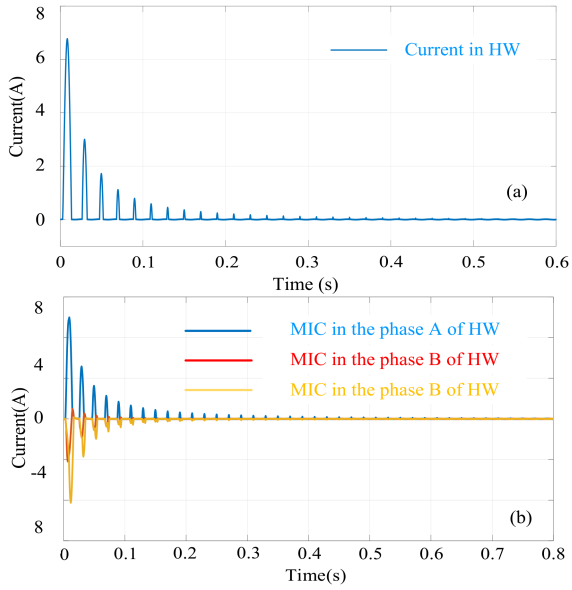

Fig. 24. Transformer primary side excitation current waveform based on series resistance of main circuit strategy. (a) Single-phase transformer. (b) Three-phase transformer.

of the transformer, whose resistance value is 100 Ω. Close the circuit breaker on the primary side of the transformer, and the MIC waveform on the primary side is shown in Fig. 24. As can be seen that the decay rate of the MIC decreases faster than that of the MIC without any measures, but this method cannot fundamentally eliminate the excitation inrush current.

According to the principle of the phase selective closing strategy, this closing strategy can completely eliminate the MIC of the power transformer in theory. However, the high-voltage circuit breaker often has a delay time, here, set the three-phase remanent magnetic $\Phi_{ra} = 0.8\Phi_m$, $\Phi_{rb} = 0$, and $\Phi_{rc} = -0.8\Phi_m$. When the phase of the transformer phase A is 150°, the circuit breaker of the phase A is closed. After 0.015 s, the circuit breaker of phases B and C is closed. At this time, the excitation current of the transformer is shown in Fig. 25. It can be seen that due to the delay time of the primary-side circuit breaker, the effect of the phase selective closing strategy on MIC suppression is not very ideal, and the delay time will have a certain influence on the peak value of the MIC.

From the comparison of the aforementioned results, it can be seen that when the asynchronous closing strategy proposed in this article is adopted, the excitation current of the primary

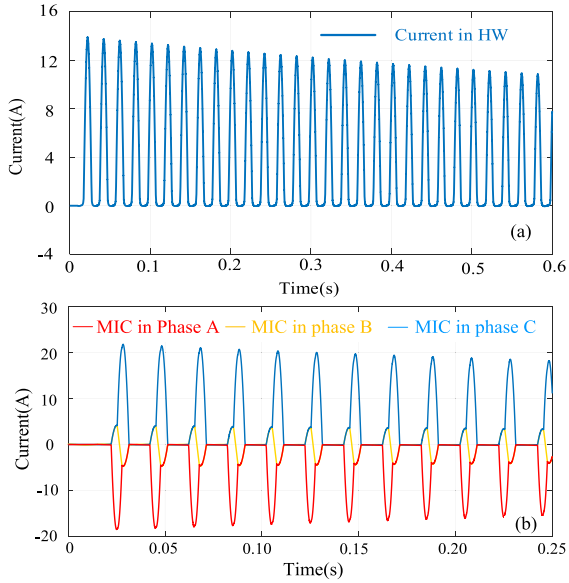

Fig. 25. Transformer primary side excitation current waveform based on phase selective closing strategy. (a) Single-phase transformer. (b) Three-phase transformer.

side of the HT directly enters the steady state, and no MIC is generated. The suppression effect of the transformer inrush current is more obvious than that of the series resistance of the main circuit strategy and the phase selective closing strategy.

VI. MIC Elimination Experiment Verification of the HT Asynchronous Closing Strategy

As the three-phase transformer is widely used in the power system, this article takes three-phase HT as an example in the MIC elimination experiment. The experimental research mainly includes the MIC simulation experiment and the asynchronous closing experiment. In order to illustrate the phenomenon clearly, the variation of the current obtained from A phase of the three-phase HT is taken as an example. The experiment system of MIC elimination contains Tektronix oscilloscope, TMS320F28335 DSP, energy storage unit, 1-kVA HT prototype, and the integrated converter circuit. The Tektronix oscilloscope is used to measure the current of the HT winding. The DSP is used to generate the signal needed for the modulated voltage. The energy storage unit serves as the input of the inverter circuit. The integrated converter outputs three-phase modulated voltage used for STMMF. The frequency of the output voltage is 50 Hz, and the effective value of the modulated sinusoidal voltage is 22 V. The steady magnetic flux is established through the AW during the experiment. When HT is connected to the grid with no load, the primary side becomes stable and does not generate MIC. The experiment site of the MIC treatment is shown in Fig. 26.

Fig. 27 shows a prototype of a step-type ac/dc modulation converter, which mainly includes the dc input, three-phase ac output, *LCL* filter, and six switching tubes. The gating signals of switches are shown in Fig. 28. When three-phase HT without load is connected to the grid, the primary-side current is collected

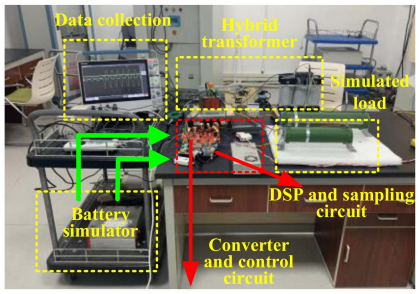

Fig. 26. MIC treatment platform.

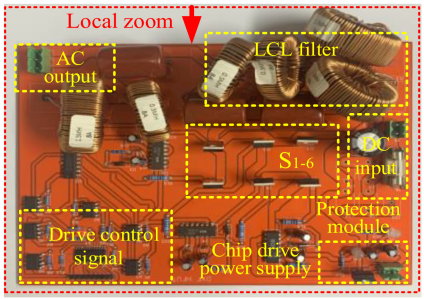

Fig. 27. Photograph of the ac/dc converter prototype.

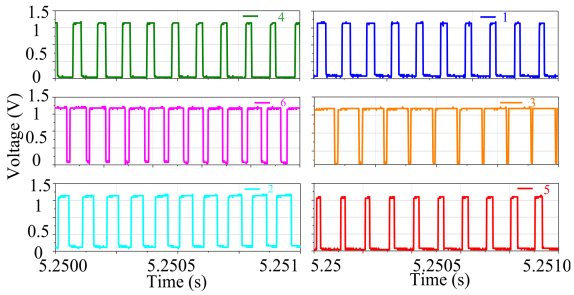

Fig. 28. Gating signals of switches S_{1-6}.

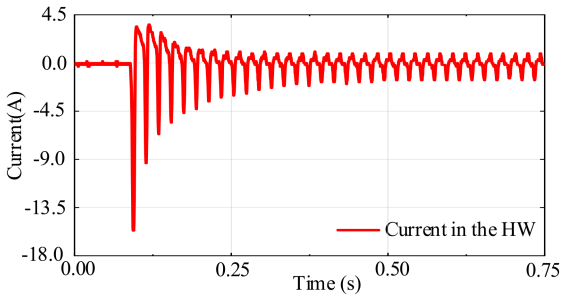

Fig. 29. Measured value of MIC at primary side of the transformer with conventional closing.

by utilizing the Tektronix oscilloscope. The current value of the primary side is shown in Fig. 29.

At 0.08 s, closing the primary-side breaker, the transformer is connected to the grid directly. From the aforementioned figure, it can be seen that the current variation of the primary side is almost same as the no-load current output of the simulation. Fig. 29 clearly shows that the primary-side excitation current value is much smaller than the simulation excitation current. There may be two reasons, one is that RM of small capacity transformer

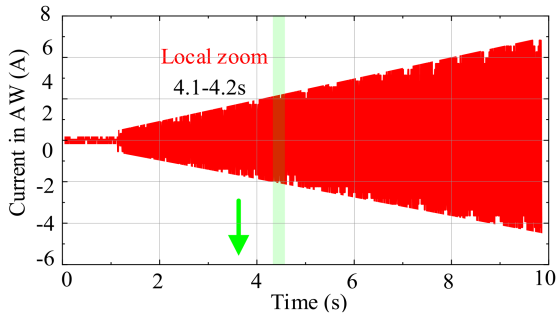

Fig. 30. Step-modulated current waveform of AW after filtering.

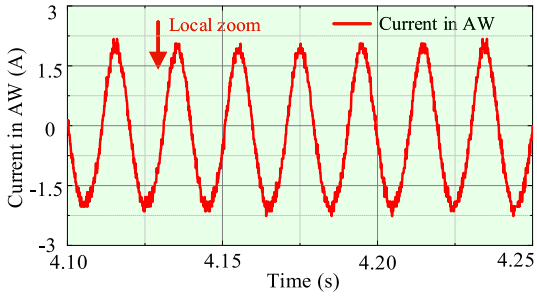

Fig. 31. Local waveform of step-modulated current in AW.

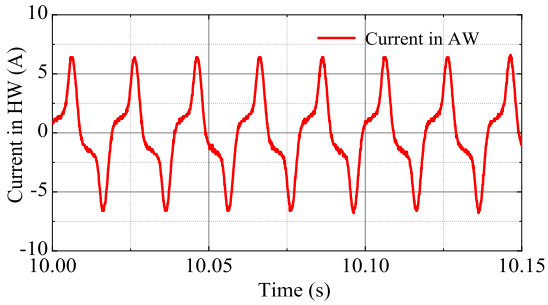

Fig. 32. Waveform distribution of step-modulated current in AW after tending to be stable.

could not achieve $0.8\Phi_m$. The other is that the direction of RM is same as the direction of the voltage induction magnetic flux, and the circuit breaker closing location is not at a maximum voltage.

For the asynchronous closing MIC elimination experiment, this article closes the AW breaker at 0 s, the voltage of AW is an alternating voltage with a step linear increase amplitude. The AW voltage reaches the rated value at 10 s, and the current of the AW gradually increases from 0 A to the rated current. Fig. 30 gives out the current waveform of AW. The current variation of the AW is slightly different from the simulation result and (10) at the beginning, and then, the current change is the same as the simulation result and (10). The reason is that RM of the transformer is uncertain. When the current of AW reaches the rated value, the STMMF is established in the iron core. The current increase and stable distribution are shown in Figs. 30 and 31. After 10s, the voltage of AW reaches into the steady value. And the current of AW also achieves the steady value. The experiment value of the AW current is shown in Fig. 32.

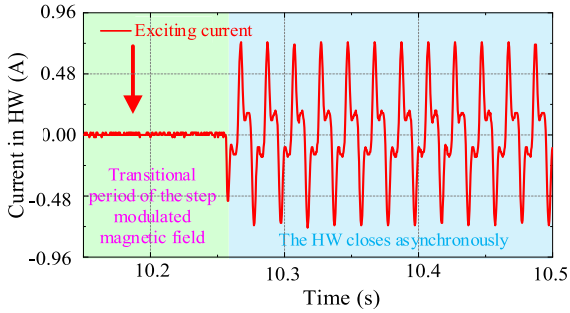

Fig. 33. Excitation current waveform during the asynchronous closing process.

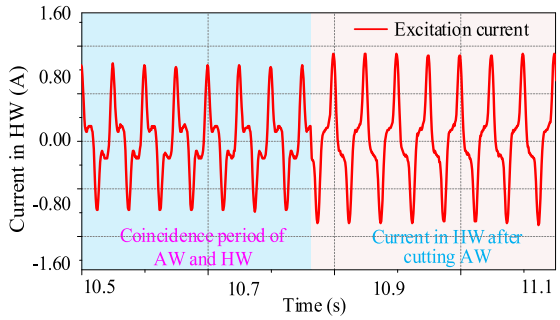

Fig. 34. Current waveform in HW after withdrawing AW.

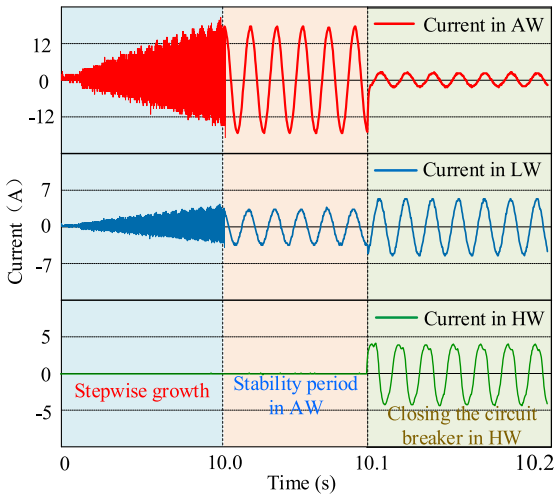

Fig. 35. Winding current change curve under transformer load closing.

When the voltage of the AW reaches the rated value, an alternating voltage nearly 220 V will be induced on the primary side. After collecting the grid phase, the circuit breaker on the primary side is selected close at 10.26 s. At this time, the primary-side current directly enters the steady state. The experimental value of the primary-side current distribution is shown in Fig. 33. By comparing the current simulation and experimental waveform, it can be found that the experimental current waveform under the asynchronous closing is consistent with the simulation results, achieving a smooth transition of the excitation current. But it can be seen that the current waveform on the right under the HW and AW together is inconsistent with that of the HW winding when the HT is unloaded, as shown in Fig. 34 (the back half),

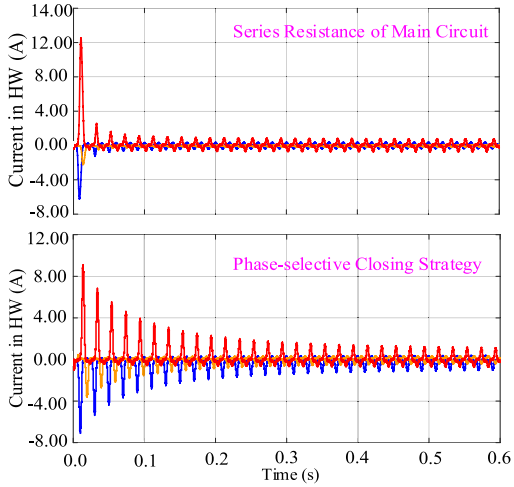

Fig. 36. Three-phase transformer primary-side excitation current waveform. (a) Series resistance of the main circuit. (b). Phase-selective closing strategy.

or the current in AW (after stabilization). This may be due to the nonlinear superposition of the excitation current in the HW and AW windings, and causing a slight current stack distortion, which does not affect the normal closing of the transformer. The experimental results show that when the stable ac flux has been established in the HT core iron, the primary-side MIC will not appear after closing the primary-side circuit breaker. At 10.80 s, the modulated voltage of the AW is withdrawn, and the variation of the primary-side current is shown in Fig. 34. When the AW is cutoff, the excitation current on the primary side of the transformer return again to the no-load state, the current tends to the normal distribution. After the AW cutting off, the current is the primary-side no-load excitation current. It can be seen that the excitation current directly enters the steady state, and no MIC is generated.

At the same time, an experimental study on the HT asynchronous closing under the load condition is conducted. In the MIC elimination experiment, a 30-Ω load resistance is connected to the LW. A modulated voltage with increasing amplitude gradually is applied on AW, and the circuit breaker on the primary side is closed at 10.1 s. The current waveform distributions of HW, LW, and AW are shown in Fig. 35. When the circuit breaker is closed, the primary current enters the steady state directly after closing the circuit breaker, and no shock current or MIC is generated. However, it should be pointed out that before the HW is closed under the load condition, a certain current component is generated in LW. It can be seen from the middle part of Fig. 35. This is because that a certain induced electromotive force can be generated by the stable modulation voltage on the LW, thereby forming a certain load current. But it does not affect the transformer closing operation, nor does it produce load shock current. After the asynchronous closing, the load running state realizes a smooth transition.

In order to illustrate the effectiveness of the proposed scheme in this article, the experiment of the MIC elimination based on the series resistance of main circuit technology and the phase selective closing strategy were conducted. Through the experimental results shown in Fig. 36, it can be found that these

two kinds of schemes have good consistency with the simulation results. Both two schemes have some shortcomings for the MIC governance, unable to completely eliminate the production of MIC, only from a certain degree, it can be alleviated and reduced, the desired effect cannot be realized. The treatment effects of these two schemes on MIC are obviously different from the elimination strategy of the asynchronous closing HT proposed in this article, as shown in Fig. 35. The effectiveness of the proposed scheme is further verified.

VII. Conclusion

A novel type of HT asynchronous closing technology for the MIC elimination scheme is proposed in this article, which does not require RM measurement, can achieve the primary-side impact-free closing. This method solves the difficulty of MIC measurement and suppression, which has broad engineering application prospects. The research results of this article are summarized as follows.

One kind of the step-type asynchronous MIC treatment scheme was designed based on the combination of the oblique signal and the sine signal. The magnetic flux of the HT iron core was derived through the differential equations theoretically. It can provide a theoretical basis for the STMMF calculation. The simulation model of single-phase and three-phase HT is designed based on the asynchronous closing strategy. The simulation results show that the MIC of the power transformer can be completely eliminated. A small capacity HT prototype was designed. The experimental platform of experiments had been carried out to verify the design scheme. The step-type modulation current was adopted as the input of the AW. The stable growth STMMF was generated by designing a reasonable slope. By connecting the primary side asynchronously to the power grid with the STMMF, the smooth transition can be realized. The generation of the MIC can be effectively restrained. The transformer without an inrush current closing can be realized, which provides a certain reference for solving the MIC of large engineering transformers.

References

[1] L. Zhou et al., "Harmonic current and inrush fault current coordinated suppression method for VSG under non-ideal grid condition," *IEEE Trans. Power Electron.*, vol. 36, no. 1, pp. 1030–1042, Jan. 2021.

[2] M. Steurer and K. Frohlich, "The impact of inrush currents on the mechanical stress of high voltage power transformer coils," *IEEE Trans. Power Del.*, vol. 17, no. 1, pp. 155–160, Jan. 2002.

[3] R. Dogan, S. Jazebi, and F. de León, "Investigation of transformer-based solutions for the reduction of inrush and phase-hop currents," *IEEE Trans. Power Electron.*, vol. 31, no. 5, pp. 3506–3516, May 2016.

[4] E. Cardelli, A. Faba, and F. Tissi, "Prediction and control of transformer inrush currents," *IEEE Trans. Magn.*, vol. 51, no. 3, Mar. 2015, Art. no. 8400304.

[5] H. Zhou, D. Li, L. He, and W. Xu, "The new synthetic loop method of ultra high voltage based on simulation research and physical experiment," in *Proc. Int. Symp. Comput., Consum. Control*, 2016, pp. 546–550.

[6] A. Wiszniewski and B. Kasztenny, "A multi-criteria differential transformer relay based on fuzzy logic," *IEEE Trans. Power Del.*, vol. 10, no. 4, pp. 1786–1792, Oct. 1995.

[7] J. Burkard and J. Biela, "Design of a protection concept for a 100-kVA hybrid transformer," *IEEE Trans. Power Electron.*, vol. 35, no. 4, pp. 3543–3557, Apr. 2020.

[8] Z. Shuai, W. Huang, C. Shen, J. Ge, and Z. J. Shen, "Characteristics and restraining method of fast transient inrush fault currents in synchronverters," *IEEE Trans. Ind. Electron.*, vol. 64, no. 9, pp. 7487–7497, Sep. 2017.

[9] M. Tajdinian and H. Samet, "Divergence distance based index for discriminating inrush and internal fault currents in power transformers," *IEEE Trans. Ind. Electron.*, vol. 69, no. 5, pp. 5287–5294, May 2022.

[10] S. K. Murugan, S. P. Simon, K. Sundareswaran, P. S. R. Nayak, and N. P. Padhy, "An empirical fourier transform-based power transformer differential protection," *IEEE Trans. Power Del.*, vol. 32, no. 1, pp. 209–218, Feb. 2017.

[11] S. Jazebi, R. Doğan, B. Kovan, and F. de León, "Reduction of inrush currents in toroidal transformers by sector winding design," *IEEE Trans. Power Electron.*, vol. 31, no. 10, pp. 6776–6780, Oct. 2016.

[12] S. R. Samantaray, "Phase-space-based fault detection in distance relaying," *IEEE Trans. Power Del.*, vol. 26, no. 1, pp. 33–41, Jan. 2011.

[13] D. Lu, Y. Yu, M. Wei, X. Li, H. Hu, and Y. Xing, "Startup control to eliminate inrush current for star-connected cascaded H-Bridge STATCOM," *IEEE Trans. Power Electron.*, vol. 37, no. 5, pp. 5995–6008, May 2022.

[14] Z. Ouyang, Z. Zhang, M. A. E. Andersen, and O. C. Thomsen, "Four quadrants integrated transformers for dual-input isolated DC–DC converters," *IEEE Trans. Power Electron.*, vol. 27, no. 6, pp. 2697–2702, Jun. 2012.

[15] S. Fang, H. Ni, H. Lin, and S. L. Ho, "A novel strategy for reducing inrush current of three-phase transformer considering residual flux," *IEEE Trans. Ind. Electron.*, vol. 63, no. 7, pp. 4442–4451, Jul. 2016.

[16] J. Fang, X. Li, X. Yang, and Y. Tang, "An integrated trap-LCL filter with reduced current harmonics for grid-connected converters under weak grid conditions," *IEEE Trans. Power Electron.*, vol. 32, no. 11, pp. 8446–8457, Nov. 2017.

[17] D. Lu, Y. Yu, M. Wei, X. Li, H. Hu, and Y. Xing, "Startup control to eliminate inrush current for star-connected cascaded H-Bridge STATCOM," *IEEE Trans. Ind. Electron.*, vol. 37, no. 5, pp. 5995–6008, May 2022.

[18] K. -H. Tan and T. -Y. Tseng, "Seamless switching and grid reconnection of microgrid using petri recurrent wavelet fuzzy neural network," *IEEE Trans. Ind. Electron.*, vol. 36, no. 10, pp. 11847–11861, Oct. 2021.

[19] S. Pugliese, G. Buticchi, R. A. Mastromauro, M. Andresen, M. Liserre, and S. Stasi, "Soft-Start procedure for a three-stage smart transformer based on dual-active bridge and cascaded H-Bridge converters," *IEEE Trans. Ind. Electron.*, vol. 35, no. 10, pp. 11039–11052, Oct. 2020.

[20] J. Burkard and J. Biela, "Design of a protection concept for a 100-kVA hybrid transformer," *IEEE Trans. Power Electron.*, vol. 35, no. 4, pp. 3543–3557, Apr. 2020.

[21] Y. Jeong, M. Park, and G. Moon, "High-Efficiency zero-voltage-switching totem-pole bridgeless rectifier with integrated inrush current limiter circuit," *IEEE Trans. Ind. Electron.*, vol. 67, no. 9, pp. 7421–7429, Sep. 2020.

Zhiwei Chen (Member, IEEE) received the Ph.D. degree in electrical engineering from the Shenyang University of Technology, Shenyang, China, in 2017.

He is currently an Associate Professor of electrical engineering with the School of Electrical Engineering and Automation, Hefei University of Technology, Hefei, China. His research interests include electromagnetic fields, electromagnetic compatibility, and design and analysis of power transformers and special electric machines.

Haonan Li received the B.S. degree in electrical engineering and automation from the Henan University of Science and Technology, Luoyang, China, in 2021. He is currently working toward the M. S. degree in electrical engineering with the Hefei University of Technology, Hefei, China.

Xiaofei Dong received the B.S. degree in electrical engineering and automation from Jiamusi University, Jiamusi, China, in 2018, and the M. S. degree in electrical engineering from the Hefei University of Technology, Hefei, China, in 2022.

Yunxiang He received the B.S. degree in electrical engineering and automation from the Harbin University of Science and Technology, Harbin, China, in 2021. He is currently working toward the M. S. degree in electrical engineering with the Hefei University of Technology, Hefei, China.

Qipei Zhou received the B.S. degree in electrical engineering and automation from China Three Gorges University, Yichang, China, in 2018. He is currently working toward the M. S. degree in electrical engineering with the Hefei University of Technology, Hefei, China.

Yujiao Zhang (Member, IEEE) received the Ph.D. degree in theory and new technology of electrical engineering from the School of Electrical Engineering, Wuhan University, Wuhan, China, in 2012.

She is currently a Professor with the School of Electrical and Automation Engineering, Hefei University of Technology, Hefei, China. Her research interests include the numerical analysis of electromagnetic field and multiphysics coupling and its application in engineering.

Yingying Zhang (Member, IEEE) received the Ph.D. degree in semiconductors and circuits from the Department of Electronics Engineering, Chungnam National University, Daejeon, South Korea, in 2010.

She is currently a Professor with the School of Electrical Engineering and Automation, Hefei University of Technology, Hefei, China. Her main research interests include power supply and distribution systems, power quality analysis and control technology, harmonic detection and suppression technology, reliability prediction, and evaluation.